Ferry Vessel Propeller Wash Effects on Scour at the Kingston Ferry Terminal, WA, USA

Sam Kastner[1]; Chris Stearns[2]; Alex Horner-Devine[3]; and Jim Thomson[4]

[1]Civil and Environmental Engineering, Univ. of Washington, Seattle, WA, USA
[2]Terminal Engineering, Washington State Ferries, Seattle, WA, USA
[3]Civil and Environmental Engineering, Univ. of Washington, Seattle, WA, USA
[4]Civil and Environmental Engineering, Univ. of Washington, Seattle, WA, USA; Applied Physics Lab, Univ. of Washington, Seattle, WA, USA

Downloaded from ascelibrary.org by Chris Stearns on 09/24/19. Copyright ASCE. For personal use only; all rights reserved.

1 ABSTRACT

Vessel propeller wash has been shown to cause scour in the marine environment. We investigated the hydrodynamic causes of severe erosion at the Washington State Ferries ferry terminal in Kingston, WA, where a cliff-like bathymetric feature has shifted shoreward in recent years, forcing repairs on the slip's bridge pilings. High resolution measurements of velocity and estimates of turbulent bed stress were made during vessel arrivals and departures during two deployment periods in March and April 2018. Calculated bed stresses were found to be 100 times larger during vessel arrivals and departures than background levels. Bed stresses were higher during vessel departures than arrivals, corresponding to higher vessel acceleration during departures. Additionally, during departures, lower tidal stages correspond to higher bed stresses, because the propellers are closer to the seabed. During arrivals, larger vessels generated higher bed stresses.

2 INTRODUCTION

The Kingston ferry terminal, in Kingston, WA (USA), has experienced rapid erosion in recent years. A steep drop at one of the slips has shifted shoreward, leading to erosion mitigation efforts. This work investigates the role of ferry-generated turbulence in causing this erosion. Specifically, we determine the magnitude of the bed stresses caused by ferry arrivals and departures compared to quiescent periods, and the dependencies of this ferry-induced bed stress on various climatological and vessel properties.

Scour, or erosion near a submerged structure, is a problem inherent to marine infrastructure [Chin et al., 1996, Hamill et al., 1998, Yuksel et al., 2012, Tan and Yuksel, 2018]. Scour occurs when turbulence near the seabed is enhanced around submerged structures, leading to significant local erosion. In the case of a bridge pile, this normally leads to a scour hole around the pile, compromising the embedment of the pile [Tan and Yuksel, 2018]. Scour due to propeller wash has been found to be a function of the wash velocity, the sediment grain size, the propeller size, and the distance of the propeller above the seabed [Tan and Yuksel, 2018].

Large vessels such as ferries create both a wake and a propeller wash, two hydrodynamic features that may contribute to scour at a ferry terminal. The vessel wake is a wave that radiates away from the vessel, while the propeller wash is turbulence generated by the vessel's propeller [Chin et al., 1996]. As a wave, the vessel wake is a smoother feature than the wash's inherently turbulent nature. The passage of a vessel involves both of these processes, and both can lead to scour [Chin et al., 1996, Hong et al., 2013].

The objective of our work is to develop a model of stress from a ferry wash in order to better predict scour at ferry terminals. We accomplish this using high resolution measurements of

turbulence at the seabed at both slips of the Kingston ferry terminal, leveraging dependencies on seabed depth, and vessel characteristics to simplify the model.

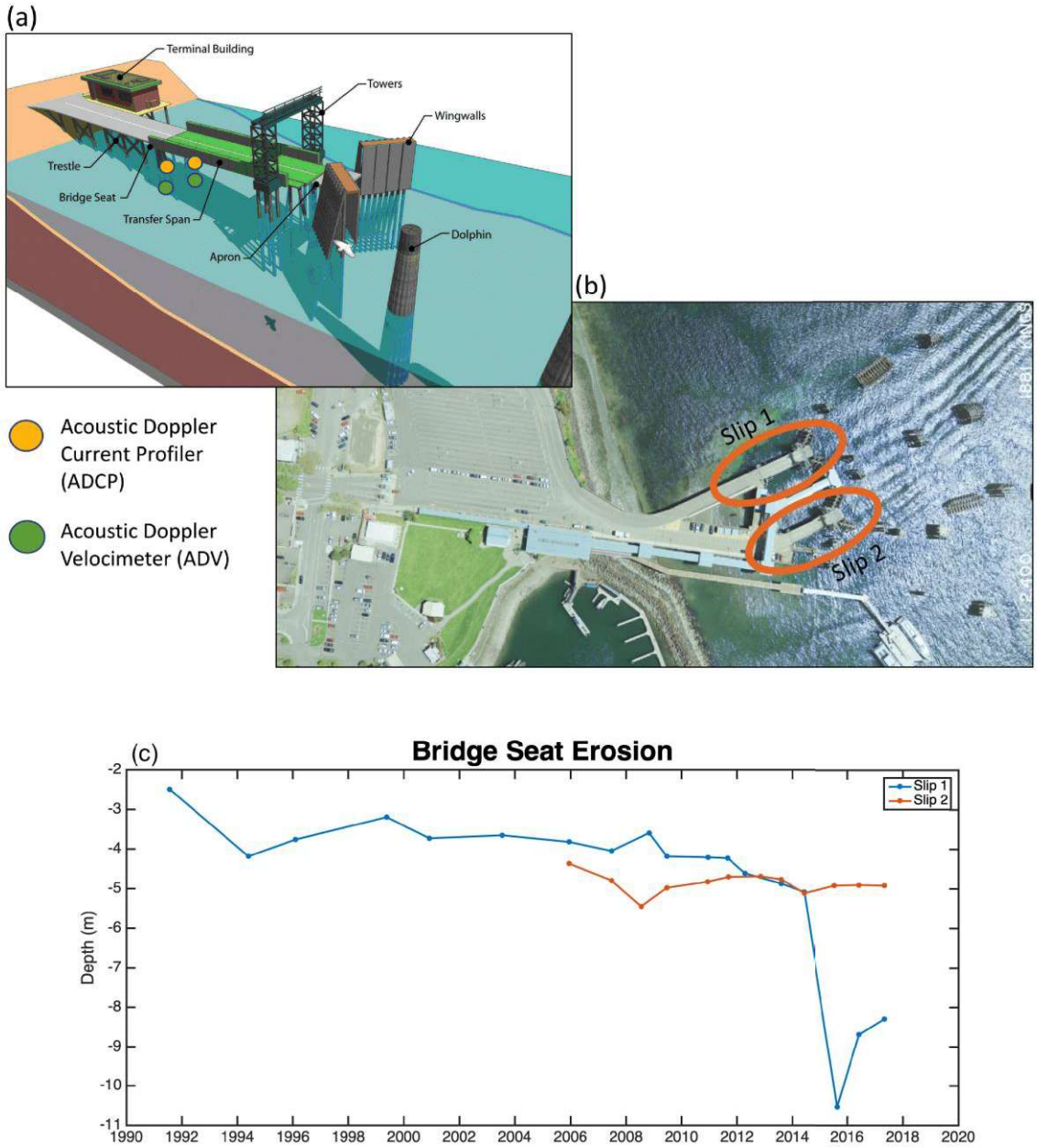

Figure 1: Experimental setup & bed elevation time series at Kingston ferry terminal, WA. (a) shows the instruments as deployed at both slips, with yellow dots corresponding to Acoustic Doppler Current Profilers at mid-depth on both bridge seat pilings, and green dots corresponding to Acoustic Doppler Velocimeters at the bottom of the same pilings; (b) shows the relative positions of Slip 1 and Slip 2 (circled in orange); (c) shows time series of erosion near the bridge seat of slip 1 (blue) and slip 2 (red).

Downloaded from ascelibrary.org by Chris Stearns on 09/24/19. Copyright ASCE. For personal use only; all rights reserved.

Downloaded from ascelibrary.org by Chris Stearns on 09/24/19. Copyright ASCE. For personal use only; all rights reserved.

3 METHODS

3.1 Observational program

Measurements were made at the Washington State Ferries, Kingston Ferry Terminal on the Puget Sound (Figure 1). The Kingston terminal has two slips. Slip 1, to the north, has a sharp cliff face directly underneath its bridge seat, and receives the most vessel traffic (Figure 1c). The sharp cliff face has eroded further shoreward on the south side of the slip than on the north side of the slip. Slip 2, to the south, has a gentler, more consistent seabed slope, and receives less vessel traffic (Figure 1c). The Kingston terminal seabed consists of cohesive sediment, with larger cobbles mixed in among finer sediment. Instrumentation packages were deployed at Slip 1 from March 15-28, 2018, and at Slip 2 from April 25-May 15, 2018. These instrumentation packages included two NorTek Vector Acoustic Doppler Velocimeters (ADVs) mounted to the base of the north and south bridge seat piles, and two NorTek Signature 1000 Acoustic Doppler 2nd generation Current Profilers (AD2CPs) mounted to the north and south bridge seat piles facing the offshore end of the slip (Figure 1). The ADVs measure velocity at a single point close to the seabed at a frequency of 16 Hz. The AD2CPs measure velocity along five 20 m long acoustic beams with measurement bins every half meter, and sampling frequency of 8 Hz. The deployment depth of each instrument varies slightly from slip to slip and piling to piling. The instruments collected data in 512 second bursts followed by 208 seconds of no collection, for a total cycle time of 12 minutes. During the period of time when a slip was instrumented, ferry traffic was redirected to that slip when possible. The analysis presented in this paper focused on the ADV data.

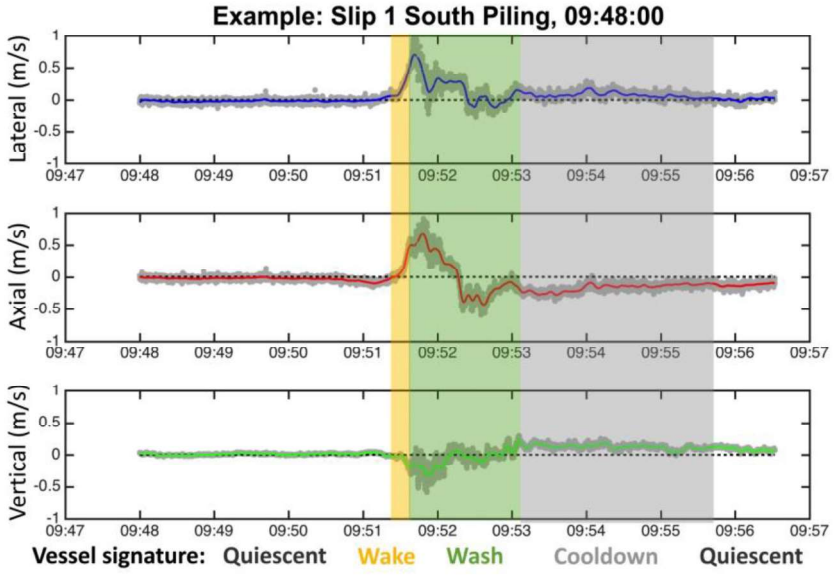

Figure 2: Example vessel arrival velocity time series from an entire data collection burst at the south piling of Slip 1. All periods are labelled. Both quiescent periods are shaded white, the wake period is shaded gold, the wash period is shaded green, and the cooldown period is shaded grey. Panel (a) shows the lateral velocity, (b) shows the axial velocity, and (c) shows the vertical velocity. Solid colored lines indicate mean velocity, while the grey shaded areas indicate the perturbations around this mean.

Downloaded from ascelibrary.org by Chris Stearns on 09/24/19. Copyright ASCE. For personal use only; all rights reserved.

Two different classes of Washington State Ferries vessels, the Jumbo and the Jumbo Mark II, were operated on the Edmonds-Kingston route during instrument deployment. The Jumbo class vessels *M/V Spokane* & *M/V Walla Walla* have displacements of 4860 long tons each, and the Jumbo Mark II class vessel *M/V Puyallup* has a displacement of 6184 long tons. The vessels are double-ended, with symmetric propulsion systems and boarding ramps on each end, allowing the vessels to arrive and depart at the terminal without changing orientation. Propeller wash is directed along the slip, as the slip-facing propeller is active for braking (arrivals) or propulsion (departures).

3.2 Vessel detection

A threshold in velocity of 50 cm/s was applied to the ADV data to determine when a vessel arrives or departs the terminal. If, during a data collection burst, any component of the velocity exceeds this threshold after the application of a low-pass filter, this burst is marked as a vessel arrival or departure. Overall, implementing the 50 cm/s threshold on data after using a low-pass filter results in very few instances of ambient conditions incorrectly labelled as arrival or departure events. Each detected event lasts 1-3 minutes, after which the vessel-induced velocity signature has diminished completely and quiescent conditions return (Figure 2). Partial events may be observed when the instruments resume their data collection period after the beginning of the arrival or departure, or if the instrument stops sampling before the end of the arrival or departure. As the initial burst of velocity is the strongest, a partial wake at the end of the data collection period could be labelled as an arrival or departure. A partial wake at the start of data collection is more likely not to be labelled an arrival or departure, as the initial burst of strong velocity occurs before the instruments have resumed data collection. Additionally, an excedence of the threshold velocity observed by the ADV on one piling, but not the other, was marked as a vessel arrival or departure for both ADVs.

3.3 Turbulence calculations

In order to calculate the turbulent stress exerted on the bed during vessel arrivals or departures, we use Reynolds' decomposition to split the axial, cross-bridge and vertical velocity components into a mean flow and a perturbation such that

$$u_i = \overline{u}_i + u_i' \tag{1}$$

where u_i is the total value of a velocity component in one of three orthogonal directions, $\overline{u_i}$ is the mean flow, and u_i' is the perturbation velocity. $\overline{u_i}$ is taken to be the low-pass filtered velocity used in smoothing the profile to detect events, and thus u'_i may be calculated such that $u_i' = u_i - \overline{u_i}$. The Reynolds stress, τ, is the stress that is generated by turbulent fluctuating velocities,

$$\tau = \rho \overline{u_i' u_j'} \tag{2}$$

where ρ is the density of the water. This formulation results from applying Reynolds' decomposition to the Navier-Stokes equations, and assumes the turbulence is isotropic and the flow is steady.

We calculate a mean Reynolds stress over the 30 seconds before and 120 seconds after the peak of the mean velocity time series during a burst, regardless of whether the mean velocity crosses the event threshold. This allows for the inclusion of the an entire arrival or departure in

the calculation, and forces the number of data points in fully captured arrivals or departures and quiescent periods to be the same. Partially captured events have fewer data points, as the record will not extend for the full 30 or 120 seconds in backward or forward in time from the peak velocity.

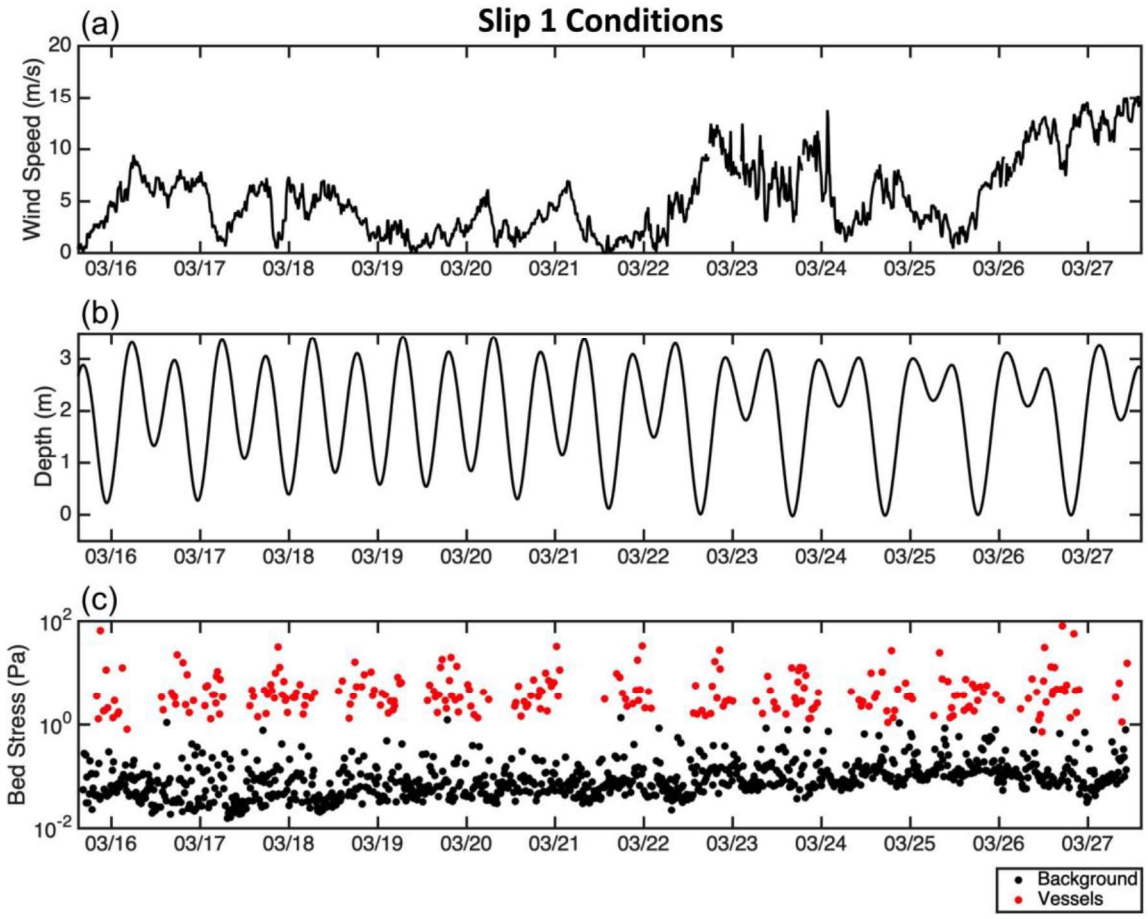

Figure 3: Climatological conditions time series during the deployment at Slip 1. Panel (a) shows wind speed; (b) shows tidal depth; (c) shows bed stress, with red points corresponding to vessel arrivals and departures and black points corresponding to bursts with no vessel activity.

4 RESULTS

4.1 Turbulent stresses at the seabed

Each deployment lasted for an entire spring-neap tidal cycle, during which wind speeds varied between 0-15 m/s, with events of over 10 m/s lasting 36 hours (Figure 3). Bed stress varies between 10^{-2} and 10^{2} Pa (Figure 3). This variability is primarily driven by vessel arrivals and departures, which are associated with bed stresses on average 100 times larger than quiescent conditions. The prolonged wind event at the end of the deployment period on Slip 1 is associated with a slight rise in the quiescent bed stress, but does not appear to have a strong influence on the bed stress associated with arrivals and departures. This indicates that adjustments made by vessel operators during strong wind conditions do not significantly

Downloaded from ascelibrary.org by Chris Stearns on 09/24/19. Copyright ASCE. For personal use only; all rights reserved.

influence the bed stress upon arrival or departure. A typical arrival or departure event has four distinct phases (Figure 2). The first and last are quiescent periods, in which background low flow conditions dominate. The second is the large mean velocity spike associated with the wake of the vessel (lasting 10-20 seconds). The wake phase is highly coherent, with minimal turbulent fluctuations (lasting 30-60 seconds). The third phase is associated with the propeller wash of the vessel; the mean velocity is smaller and turbulent fluctuations are large (lasting 1 minute). The last phase is a cooldown period, over which time both the mean velocity and the turbulent fluctuations decay to quiescent levels. The largest mean velocities occur in the along-slip component, followed by the cross-slip component, and then the vertical component.

In general, a higher value of maximum velocity during a data collection burst corresponds to a higher bed stress (not shown). This is true for arrivals, departures, and quiescent periods. It is known that the propeller wash is the dominant source of turbulence close to a vessel, consistent with our result that the propeller wash contains larger fluctuations than the wake [Chin et al., 1996]. However, the positive correlation between the maximum velocity and the bed stress observed during a data collection burst implies that the speed of the wake and the turbulent intensity of the wash are linked. Thus, the initial velocity spike due to the wake of an arrival or departure does not directly cause high bed stress, but is instead associated with a larger bed stress due to the subsequent propeller wash.

The vessel arrival and departure bed stresses vary in magnitude from 1 to 100 Pa. This variability is not explained by wind or tidal forcing. One contributing factor to this variability is the difference in the bed stress associated with vessel arrivals and departures. Vessel arrivals are generally associated with lower bed stresses than vessel departures (Table 1) at the south pilings of both slips, with similar stresses at the north pilings. The difference at the south pilings could be due to deceleration during arrivals being smaller than acceleration during departures and directionality of the propeller wash (addressed in section 5.3).

Table 1: Mean stresses at both slips for both pilings, and sensor deployment depths relative to mean lower low water.

Location		Mean Stresses (Pa)			Sensor Depth (m)
Slip	Piling	All	Arrivals	Departures	
1	North	3.6	4.0	3.7	9.8
1	South	6	4.8	5.6	5.9
2	North	3.6	3.6	3.5	4.2
2	South	3.9	3.6	4.2	5.1

4.2 Depth Dependence

As water level at the ferry terminal oscillates due to the tide, vessel arrivals and departures occur at varying water levels. Intuition would suggest that at lower water levels bed stress would be higher, as the propeller is closer to the seabed. However, this is not always the case. Vessel departures are associated with a strong relationship of bed stress with depth (Figure 4), while vessel arrivals do not (not shown). Figure 4 shows the relationship between depth and bed stress for departures at slip 1. Bed stress data were bin averaged by depth before fitting, disregarding depth bins with a low number of measurements. During vessel departures, tidal elevation is the primary source of variability in the observed bed stress; at lower water levels, higher bed stresses occur (Figure 4). There is no observable relationship between bed stress and depth for vessel arrivals at either piling of either slip (not shown). It is possible that the high acceleration during departures advects the propeller wash to the seabed. During arrivals, however, the lower

Downloaded from ascelibrary.org by Chris Stearns on 09/24/19. Copyright ASCE. For personal use only; all rights reserved.

deceleration results in a more diffusive process which results in the turbulence decaying to a consistent level before it reaches the seabed.

4.3 Vessel Dependence

The two classes of vessels operating during the measurements differed in displacement, with the Jumbo Mark II class *M/V Puyallup* displacing 50% more than the Jumbo class *M/Vs Walla Walla* and *Spokane*. As more thrust is necessary to change the speed of a larger vessel, it would follow that the acceleration and deceleration behaviors of different vessel types are different. The disparity in vessel size results in higher bed stress during *Puyallup* arrivals than *Spokane* or *Walla Walla* arrivals (Figure 5). This relationship between displacement and bed stress is not observed during vessel departures (not shown). Different acceleration and deceleration behaviors between arrivals and departures for different vessel classes could account for the lack of relationship between vessel size and bed stress upon vessel departure. It is important to note that the *Puyallup* was used less frequently than either the *Spokane* or *Walla Walla* during the study period.

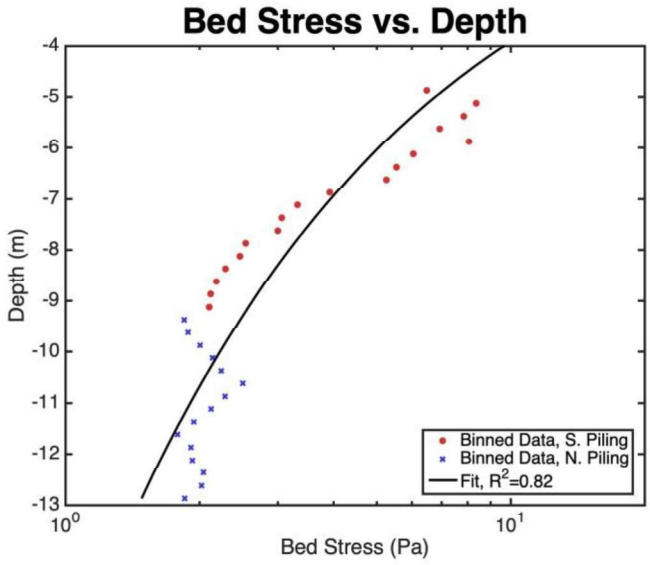

Figure 4: Profiles of bed stress at varying depths for departures at slip 1. The binned data is shown as colored points (red crosses for the north piling, blue circles for the south) and the fit is shown as a solid black line with an R^2 value given in the legend.

5 DISCUSSION

5.1 A simple model for vessel scour potential at the seabed

The overall objective of this work is to develop a predictive understanding for the scour due to ferry propeller wash. Our turbulence data show that the prop wash depends strongly on the water depth and also on the lateral location of the measurement. This is consistent with a conceptual picture of the prop wash as a turbulent jet extending back from the vessel to the pilings, whose intensity decreases vertically and horizontally away from the main axis of the jet. Engineering jets are often modeled with a Gaussian structure that accounts for the attributes listed above. In order to generate a predictor for the scour potential due to bed stress from the prop wash, we fit our bed stress measurements to a Gaussian model. We choose vessel

Downloaded from ascelibrary.org by Chris Stearns on 09/24/19. Copyright ASCE. For personal use only; all rights reserved.

departures because departures are associated with higher stresses and show stronger spatial dependence. We assume the turbulent wash exhibits a Gaussian profile in depth and across-slip distance, as is common for turbulent jets. The wash can then be modeled by the equation

$$\tau = \alpha e^{-\left(\frac{y-y_0}{\sigma_y}\right)^2} e^{-\left(\frac{z-D_p}{\sigma_z}\right)^2}, \quad (3)$$

where α is a constant source term in Pascals, y is across-slip distance, y_0 is the across-slip location of the maximum stress, σ_y is a measure of the spread of stress with across-slip distance z is the depth of the bed, D_p is the depth of the vessel propeller, and σ_z is a measure of the spread of stress with depth. The details of model calculations are described in Appendix A.

Using this model allows us to determine the spatial characteristics of an average vessel departure wash. The structure of the wash is governed by the spread parameters, σ_y and σ_z. These represent, in a physical sense, how strongly the turbulence advects and diffuses away from the propeller horizontally and vertically. The strength of the wash is governed by the source term α, which scales the rest of the relationship. The wash strength is independent of the wash geometry, and is thus a function of only vessel characteristics. For this model, we will fit α empirically. In reality, α likely depends on the force the vessel exerts on the water as it arrives at or departs the slip. Thus, this model gives insight into the strength of the wash and its across-slip spatial distribution between the two pilings.

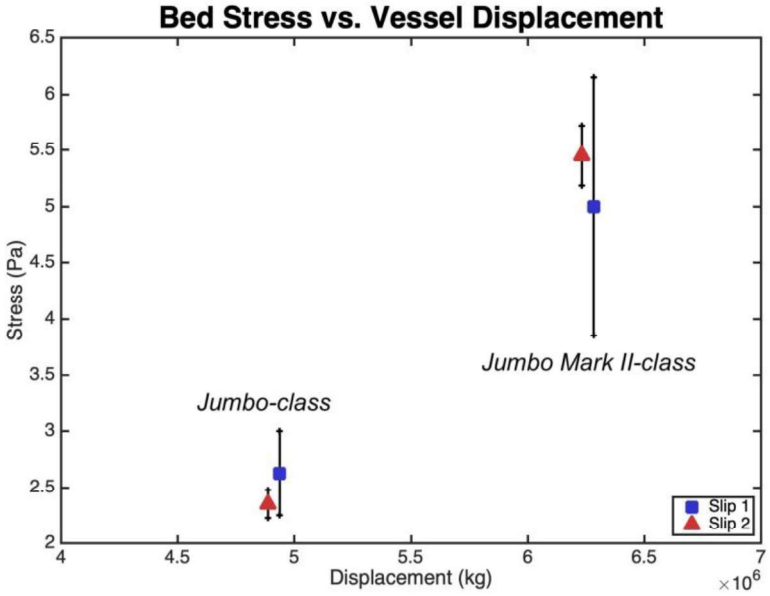

Figure 5: Bed stress by vessel displacement, averaged over both pilings at each slip. Slip 1 values are shown by blue squares, slip 2 values by red triangles. Whiskers show standard error bounds. Each vessel in a vessel class has the same displacement. The apparent small difference in displacement between slips is for legibility only and does not reflect actual differences in vessel displacement.

This model shows good skill at reproducing the stress profiles at each piling, particularly for smaller depths. It captures the horizontal variability of the stress well, and does well vertically to approximately 9 m depth. Deeper than this, the model under-predicts the stress observed. It should be noted that this deeper stress data comes only from the north piling of Slip 1, at the bottom of the cliff face. It is possible that the stress is enhanced at this location due to self-

Downloaded from ascelibrary.org by Chris Stearns on 09/24/19. Copyright ASCE. For personal use only; all rights reserved.

advection of the turbulence down the cliff face.

This simple model may be used to predict the expected stress at variable horizontal locations on the seabed, for variable depth. It does not depend on local bathymetry, and so it is portable to other Washington State Ferries terminals. Calibrated for other vessels, it can also provide information about scour potential in other ferry and vessel systems. It is important to note that this version of the model, with a constant α, is only valid when depth dependence is more important than vessel class dependence. When vessel class dependence dominates, α will need to be variable to account for the influence of the varying mass of the vessel. Figure 5 provides preliminary estimates of how much α might change between vessels of differing displacement.

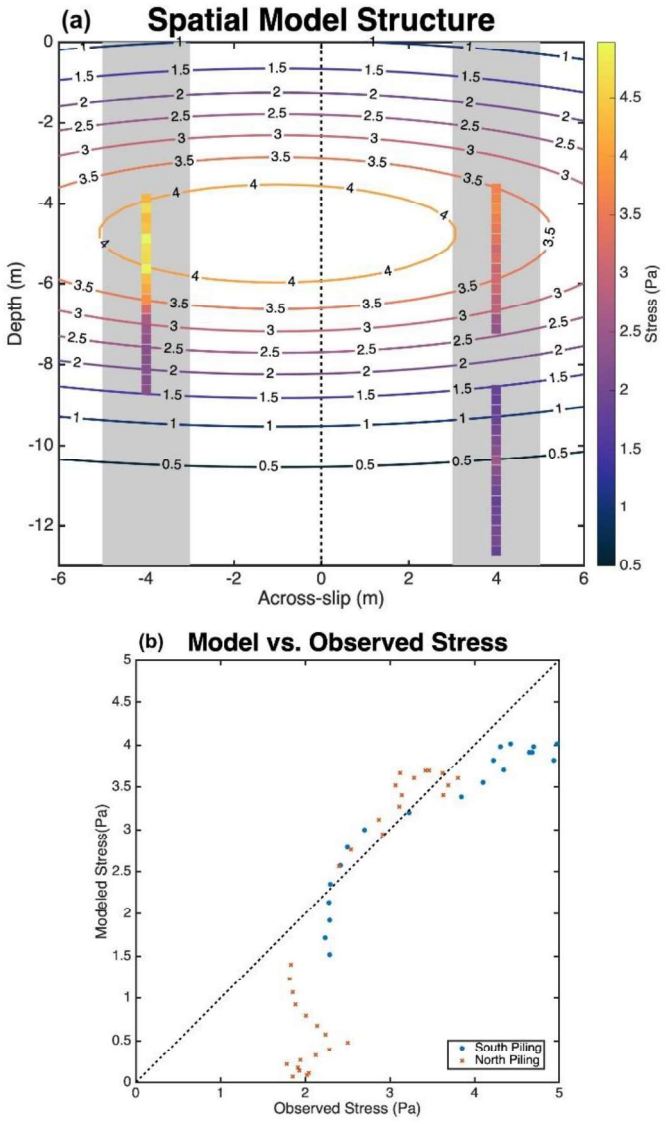

Figure 6: (a) shows the spatial variability of model results as contours of constant stress (in Pa) and the depth profiles of stress at each piling as a colored square (using the same color scale as the contours, shown by the color bar). The grey shaded regions are the approximate locations of the pilings, and the black dashed line is the centerline of the slip. (b) shows the observed vs. modelled stresses at the south and north pilings. The dashed black line shows the 1:1 line.

Downloaded from ascelibrary.org by Chris Stearns on 09/24/19. Copyright ASCE. For personal use only; all rights reserved.

It is important to note that this model predicts bed stress, not scour. Predictions of scour require information about the seabed sediment in addition to the applied stress. Relationships between stress and scour may be developed for this or other sites based on observations of stress and scour taken over longer time periods, or may be adopted from studies of scour in rivers or other coastal settings.

5.2 Sediment Transport

While the current measurements do not address scour directly, it is worth considering how the observed stress magnitudes are expected to influence the bed. We start by considering initiation of motion, based here on thresholds described, for example, in Shields [1936] and Julien [2010]. The stresses observed during vessel arrivals and departures are 5 Pa, large enough to move fine to medium gravel ($\sim$ 8 mm diameter). The largest bed stresses observed are greater than 40 Pa, large enough to move very coarse gravel ($\sim$ 5 cm diameter). The bed stresses during events vary between 1 and 100 Pa, while the stresses during quiescent periods are mostly lower than 0.5 Pa, moving very coarse sand ($\sim$ 1 mm diameter) at maximum. The mean quiescent bed stress is 0.25 Pa, corresponding to the threshold stress for medium sand ($\sim$ 0.25 mm diameter). This relationship between bed stress and particle size assumes a horizontal seabed, and so it is likely that larger particles will be mobilized given the slope of the seabed, particularly for the cliff face at Slip 1. Thus, the large mean bed stresses during departures and arrivals are almost certainly strong enough to initiate motion among the small particles at the seabed, and the maximum stresses are large enough to initiate motion amount the large cobbles embedded within the smaller particles. This could lead to two modes of erosion: the gradual erosion of smaller particles around an embedded larger cobble by average vessel-induced stresses until the cobble is able to fall away from the rest of the seabed, or the direct removal of cobbles by vessel-induced stresses close to the maximum observed.

Previous laboratory experiments on scour due to propeller washes have found that scour depends many hydrodynamic parameters, including the depth of the propeller, the distance between the propeller and the seabed, the grain size of the sediment at the seabed and the velocity of the propeller wash [Hong et al., 2013, Tan and Yuksel, 2018, Yuksel et al., 2018]. Based on our analysis, we observe dependence on similar quantities: the water depth and the size of the vessel, which are analogous to the seabed-propeller distance and the initial velocity of the propeller wash, respectively. However, our analysis uses direct calculations of bed stress as opposed to the properties of the propeller wash jet used in the experimental studies of Yuksel et al. [2018]. Future work will make use of the 5-beam AD2CP data to directly estimate the flux velocity of the propeller wash jet, in order to directly compare the bed stresses we observe with the experimental scour results.

5.3 Inter-piling and inter-slip variability

Bed stress varies both between the pilings on a particular slip for a given arrival or departure, and between slips. In particular, stresses are slightly higher at Slip 1 than Slip 2 (see Table 1). This is opposite from expected trends, as the seabed (where the ADVs were deployed) is deeper at Slip 1 than at Slip 2, and thus father from the propeller. There must, then, exist a different mechanism for the advection of propeller wash turbulence to the seabed at Slip 1 than at Slip 2. Since the two slips have different bathymetry, with Slip 1 having a shear cliff face and Slip 2 a gentle slope, we posit that the turbulence either self-advects down or reflects off the cliff face.

Downloaded from ascelibrary.org by Chris Stearns on 09/24/19. Copyright ASCE. For personal use only; all rights reserved.

Such a process could result in more intense turbulence at the seabed, leading in turn to higher bed stresses.

The bed stresses during vessel arrivals and departures at the south pilings of both slips are higher than at the north pilings (Table 1). This likely indicates that there is a southern preference in the direction of the propeller wash (as seen in the model), as the higher stress indicates that turbulence is more energetic at the south piling, and thus has not had as much time to diffuse. The lack of clarity in a signal between arrivals and departures at the north pilings support the conceptual picture of the propeller wash being directed at the south piling before diffusing to the north, as this could result in similar signals at the north piling due to diffusion of turbulence. A southerly directed wash would help explain the spatial pattern of erosion in the cliff face at Slip 1, as this directionality could con- ceivably cause stronger seabed erosion at the southern piling. It is important to note that the large difference between the south and north pilings at Slip 1 must be partially due to the large difference in depth between the two ADVs (Table 1). The rotational direction of the vessels' propellers might drive preferential self-advection of the propeller wash toward the south, resulting in these higher bed stresses.

6 SUMMARY AND FUTURE WORK

Vessel arrivals and departures cause high bed stresses at the seabed of both slips at the Kingston, WA ferry terminal. These bed stresses are $\sim 100\times$ larger than background stresses due to the turbulent nature of the ferry propeller wash. Furthermore, vessel departures have higher associated bed stresses than vessel arrivals, and vessel departures at lower tidal stages cause higher bed stress than those at higher tidal stages. The higher stress upon vessel departure is likely due to larger accelerations during departure than arrival. Vessel arrivals do not show a depth dependence, but larger vessel displacement is associated with higher bed stress during arrivals. Thus, the largest vessel-influenced bed stresses occur during vessel departures at low water, and the lowest vessel-influenced bed stresses occur during the arrivals of smaller vessels. An empirical model of bed stress during departures replicates this behavior.

Future work will focus on refining the simple stress model presented above and characterizing the three dimensional wash structure using 5-beam AD2CP measurements, with a focus on understanding the wash directionality. The rotational and radial components of propeller wash velocity fields are not currently well understood [Lam et al., 2010]. Expanding the model to include information about stress dependence on vessel mass during arrivals will allow predictions of bed stress exposure for a given ferry terminal using historical data of vessel class, tidal stage, and the dependencies demonstrated in this work.

A APPENDIX: MODEL METHODS

The model in equation 3 is separable into y and z equations, such that a regression can be performed with respect to both across-slip distance and depth in a log-linear sense. We use the ADV data to perform this regression, combining measurements from both slips to produce a profile of stress with depth for the south and north pilings. The spread between the pilings is approximately 8 m, and so the north and south pilings have a position of 4 and -4 m respectively. This coordinate system places the origin in the center of the bridge span at the water surface. We first fit α and σ_z using the z term and the ADV depth and bed stress data. We then take into account this value of α to fit σ_y to the the piling positions and ADV ved stress data, forcing the intercept of the across-slip fit through the origin. The parameters D_p and y_0 are not addressed by the fit, and must be chosen manually. D_p would be equal to the depth of the propeller for a model

Downloaded from ascelibrary.org by Chris Stearns on 09/24/19. Copyright ASCE. For personal use only; all rights reserved.

of stress at the propeller's location, but since the pilings are located shoreward of the propeller, we take D_p as equal to the depth of maximum stress in the south piling stress profile, $D_p = 5$ m. y_0 must be negative (closer to the south piling) because of the higher stresses and correlations with depth at the south pilings, and so we choose a y_0 such that the model fits the calculated stress profiles reasonably well, $y_0 = -1$ m (Figure 6). We further observe that the fitted value of σ_y underpredicts the spread seen between the depth profiles at each piling. In Figure 6, we multiply σ_y by a factor of 2, which compensates for this difference. We thus calculate $\alpha = 4.4$ Pa, $\sigma_y = 13.1$ m, and $\sigma_z = 3.9$ m.

REFERENCES

C. Chin, Y. Chiew, S. Y. Lim, and F. H. Lim. Jet scour around vertical pile. *J. Waterway, Port, Coastal, Ocean Eng.*, 122(2):59–67, 1996. doi: https://doi.org/10.1061/(ASCE)0733-950X(1996)122:2(59).

G. A. Hamill, J. A. McGarvey, and P. A. Mackinnon. A method for estimating the bed velocities produced by a ship's propeller wash influenced by a rudder. *Coastal Engineering Proceedings*, 1(26), 1998. URL https://icce-ojs-tamu.tdl.org/icce/index.php/icce/article/view/5867.

J. H. Hong, Y. M. Chiew, and C. N. S. Scour caused by a propeller jet. *Journal of Hydraulic Engineering*, 139(9):1003–1012, 2013. doi: 10.1061/(ASCE)HY.1943-7900.0000746.

P. Julien. *Erosion and Sedimentation*. Cambridge University Press, 2nd edition, 2010. ISBN 978-0-521- 83038-6.

W. Lam, G. A. Hamill, Y. C. Song, D. J. Robinson, and S. Raghunathan. A review of the equations used to predict the velocity distribution within a ship's propeller jet. *Ocean Engineering*, 38(1):1–10, 2010. doi: https://doi.org/10.1016/j.oceaneng.2010.10.016.

A. Shields. *Application of similarity principles and turbulence research to bed-load movement*. PhD thesis, T.U. Delft, 1936. URL http://resolver.tudelft.nl/uuid:a66ea380-ffa3-449b-b59f-38a35b2c6658. Translation of the Ph.D. thesis of A. Shields, 'Anwendung der Aehnlichkeitsmechanik und der Turbulenzforschung auf die Geschiebebewegung'.

R. I. Tan and Y. Yuksel. Seabed scour induced by a propeller jet. *Ocean Engineering*, 160:132–142, 2018. doi: https://doi.org/10.1016/j.oceaneng.2018.04.076.

Y. Yuksel, S. Kayhan, Y. Celikoglu, and K. Cihan. Open type quay structures under propeller jets. *Coastal Engineering Proceedings*, 1(33), 2012. URL https://icce-ojs-tamu.tdl.org/icce/index.php/icce/article/view/6468.

Y. Yuksel, R. I. Tan, and Y. Celikoglu. Propeller jet flow around a pile structure. *Applied Ocean Research*, 79:160–172, 2018. doi: https://doi.org/10.1016/j.apor.2018.08.001.

Downloaded from ascelibrary.org by Chris Stearns on 09/24/19. Copyright ASCE. For personal use only; all rights reserved.